Pergamon

Int. J. Multiphase Flow Vol. 22, No. 2, pp. 363–377, 1996

0301-9322(95)00073-9
0301-9322/96 $15.00 + 0.00

INSTABILITY OF A TWO-LAYER CAPILLARY JET

V. Ya. SHKADOV and G. M. SISOEV
Department of Mechanics and Mathematics, Moscow State University, Moscow 119899, Russia

(Received 13 February 1994; in revised form 20 October 1995)

Abstract—An axisymmetrical flow of a two-layer capillary jet is studied. The most general formulation of the jet instability problem is considered. The influence of the governing parameters on the amplification factor of the disturbances is investigated taking into account the variation along the jet of the main flow velocity profile. The boundary layer approximation to full Navier–Stokes formulation is applied for calculation of a stationary mean flow. Stability analysis is carried out for various cross sections along the jet on the assumption of a locally parallel main flow.

Numerical calculations of the corresponding eigenvalue problem reveal two types of unstable perturbations connected with the presence of the free surface and interface accordingly. The predominant type of instability is defined by the main flow properties. Numerous solutions of the multiparameter stability problem are presented.

Key Words: hydrodynamic instability, two-layer capillary jet, axisymmetrical flow, viscous fluids

1. INTRODUCTION

In connection with the application of two-layer capillary jets in color printers, Hertz & Hermanrud (1983) have carried out the most complete experimental studies of this flow. Their results have stimulated further theoretical investigations.

Radev & Shkadov (1985) applied the one-dimensional inviscid approximation of Markova & Shkadov (1972) to the stability analysis of two-layer jets. The asymptotic analysis of the dispersion equation revealed the existence of two unstable modes which relate to the interface and the free surface accordingly. The surface type modes are more unstable than the interface ones for the cases considered. Various possible regimes of jet breaking have been discussed on the basis of linear stability analysis. Similar results have been obtained numerically in Sanz & Meseguer (1985).

In Kamenov & Radev (1987) a two-dimensional inviscid model was applied. Results of the considered asymptotic cases are the same as in Radev & Shkadov (1985). It may be noted that numerical analysis of the dispersion equation leads to the discovery of main flows with two local maxima of the amplification factor curve for surface type perturbations.

Stability analysis of a viscous compound jet has been carried out in Kamenov & Radev (1988) and Radev & Tchavdarov (1988). At large Reynolds numbers the results of viscous and inviscid stability analyses were shown to be very close for the jet flows with a uniform main flow velocity profile. Some limiting cases of the dispersion equation for such compound jet flows have been considered in Petryanov-Sokolov & Shutov (1984) and Shutov (1985), without quantitative analysis of each type of unstable perturbation.

Epikhin & Shkadov (1978) have shown that radial variations of the main flow velocity had a strong effect on the amplification factors for the case of a capillary jet interacting with its surroundings. The velocity variations at the initial part of the compound jets of Hertz & Hermanrud's (1983) experiments are essential. To carry out stability analysis for such cases it is necessary to take into account the main flow variations.

A numerical method for calculation of the developing axisymmetric jet flow has been offered in Shkadov (1973) for flows with one unknown free surface. This method is based on the boundary layer approximation to full Navier–Stokes formulation. In Epikhin *et al.* (1989a,b), a generalization for flows with a free surface and interface has been carried out. This method is used in the presented work. Radev & Gospodinov (1986) have used the transformation of boundary layer equations to Protean coordinates as a generalization of Duda & Vrentas' (1967) method. The survey of Shkadov *et al.* (1982) contains a detailed discussion of the numerical methods for single-layer jets.

Complete formulation of the stability problem, taking into account the effects of the radial and longitudinal velocity variations for compound jets, is presented in this paper. All previously mentioned articles may be considered as special cases of this formulation. Section 2 contains the basic equation and boundary conditions formulation, stationary axisymmetric compound jet flows are investigated in section 3 and section 4 contains the stability analysis. Discussion of the numerical results is given in section 5.

2. BASIC EQUATIONS

Let the capillary jet consist of two layers of immiscible viscous fluids. For the flow description we introduce the cylindrical coordinate system r, θ, z in which the origin is located at the center of some initial jet section and the axis z is directed along a jet flow. The scales of mean length and velocity are R_c and U_c, and R_c is the radius of the initial section and $U_c = Q/(\pi R_c^2)$, Q being the volume rate of a jet. Dimensionless values are defined as

$$r = R_c y, \quad z = R_c x, \quad T = \frac{R_c}{U_c} t,$$

$$u_z = U_c u, \quad u_r = U_c v, \quad p_f = \rho^{(1)} U_c^2 p, \quad h_f^{(1)} = R_c h^{(1)}, \quad h_f^{(2)} = R_c h^{(2)}$$

where T is time, u_r and u_z are radial and axial velocities, p_f is pressure, $h_f^{(1)}$ and $h_f^{(2)}$ are the radii of the interface and surface, and $\rho^{(1)}$ is the density of the first liquid (we use a superscript 1 for values corresponding to the inside layer and a superscript 2 for values of the outward layer). The scales making provides the unit dimensionless rate of a jet.

For axisymmetric flows the Navier–Stokes equations are

$$y\frac{\partial u}{\partial x} + \frac{\partial (yv)}{\partial y} = 0,$$

$$\frac{\partial u}{\partial t} + u\frac{\partial u}{\partial x} + v\frac{\partial u}{\partial y} = -\frac{1}{\rho_0^{(j)}}\frac{\partial p}{\partial x} + \frac{v_0^{(j)}}{\mathrm{Re}}\left(\frac{\partial^2 u}{\partial x^2} + \frac{\partial^2 u}{\partial y^2} + \frac{1}{y}\frac{\partial u}{\partial y}\right) + \frac{1}{\mathrm{Fr}^2},$$

$$\frac{\partial v}{\partial t} + u\frac{\partial v}{\partial x} + v\frac{\partial v}{\partial y} = -\frac{1}{\rho_0^{(j)}}\frac{\partial p}{\partial y} + \frac{v_0^{(j)}}{\mathrm{Re}}\left(\frac{\partial^2 v}{\partial x^2} + \frac{\partial^2 v}{\partial y^2} + \frac{1}{y}\frac{\partial v}{\partial y} - \frac{v}{y^2}\right), \quad j = 1, 2 \qquad [1]$$

where $\rho_0^{(1)} = v_0^{(1)} = 1$, $\rho_0^{(2)} = \rho_0 \equiv \rho^{(2)}/\rho^{(1)}$, $v_0^{(2)} = v_0 \equiv v^{(2)}/v^{(1)}$, $\rho^{(j)}$ and $v^{(j)}$ are the densities and viscosities of the fluids, $\mathrm{Re} = U_c R_c / v^{(1)}$, $\mathrm{Fr} = U_c/\sqrt{gR_c}$ and g is the acceleration due to gravity. The case $\mathrm{Fr} = \infty$ corresponds to a jet flow without an external mass force.

The boundary conditions at the interface ($y = h^{(1)}$) include the kinematic equation, the continuity of the velocity components and the tangential stresses and the condition for normal stresses in layers taking into account the stress induced by the interface tension $\sigma^{(1)}$

$$\frac{\partial h^{(1)}}{\partial t} + u\frac{\partial h^{(1)}}{\partial x} = v, \quad [u]_1^2 = 0, \quad [v]_1^2 = 0, \qquad [2]$$

$$[\rho_0^{(j)} v_0^{(j)} p_{nr}]_1^2 = 0, \quad [p_{nn}]_1^2 + \frac{\kappa}{\mathrm{We}} = 0;$$

where $\mathrm{We} = \rho^{(1)} U_c^2 R_c / \sigma^{(1)}$. In [2] the notation $[s]_1^2 = s^{(2)} - s^{(1)}$ is used. The expressions for stresses p_{nn}, p_{nr} and curvature κ are determined as

$$p_{nr} = \frac{1}{d^2}\left\{\left[1 - \left(\frac{\partial h^{(1)}}{\partial x}\right)^2\right]\left(\frac{\partial u}{\partial y} + \frac{\partial v}{\partial x}\right) - 2\frac{\partial h^{(1)}}{\partial x}\left(\frac{\partial u}{\partial x} - \frac{\partial v}{\partial y}\right)\right\},$$

$$p_{nn} = -p + \frac{2\rho_0^{(j)} v_0^{(j)}}{\mathrm{Re}\, d^2}\left[\frac{\partial v}{\partial y} - \frac{\partial h^{(1)}}{\partial x}\left(\frac{\partial v}{\partial x} + \frac{\partial u}{\partial y} - \frac{\partial h^{(1)}}{\partial x}\frac{\partial u}{\partial x}\right)\right],$$

$$\kappa = \frac{1}{d^3}\left(\frac{\partial^2 h^{(1)}}{\partial x^2} - \frac{d^2}{h^{(1)}}\right), \quad d^2 = 1 - \left(\frac{\partial h^{(1)}}{\partial x}\right). \qquad [3]$$

At the free surface ($y = h^{(2)}$) the radius $h^{(2)}$ is related to the velocity by the kinematic equation, the tangential stress must vanish and the normal stress is balanced by the stress induced by the surface tension $\sigma^{(2)}$

$$\frac{\partial h^{(2)}}{\partial t} + u\frac{\partial h^{(2)}}{\partial x} = v, \quad p_{n\tau} = 0, \quad p_{nn} - \frac{\sigma_0 \kappa}{We} = 0 \qquad [4]$$

where $\sigma_0 = \sigma^{(2)}/\sigma^{(1)}$ and the expressions for $p_{n\tau}, p_{nn}$ and κ are similar [3].

3. A STATIONARY AXISYMMETRIC FLOW

To define a stationary axisymmetric jet flow an approximate system of equations and boundary conditions is used, see Shkadov *et al.* (1982) and Epikhin *et al.* (1989a,b)

$$y\frac{\partial U}{\partial x} + \frac{\partial (yV)}{\partial y} = 0,$$

$$U\frac{\partial U}{\partial x} + V\frac{\partial U}{\partial y} = \frac{v_0^{(j)}}{Re}\left(\frac{\partial^2 U}{\partial y^2} + \frac{1}{y}\frac{\partial U}{\partial y}\right) + \frac{1}{Fr^2} + F^{(j)}, \quad j = 1, 2,$$

$$F^{(1)} = \frac{1}{We}\left(\frac{1}{(H^{(1)})^2}\frac{dH^{(1)}}{dx} + \frac{\sigma_0}{(H^{(2)})^2}\frac{dH^{(2)}}{dx}\right), \quad F^{(2)} = \frac{\sigma_0}{\rho_0 We (H^{(2)})^2}\frac{dH^{(2)}}{dx};$$

$$y = 0: \quad \frac{\partial U}{\partial y} = 0, \quad V = 0;$$

$$y = H^{(1)}: \quad U\frac{dH^{(1)}}{dx} = V, \quad [U]_1^2 = 0, \quad [V]_1^2 = 0, \quad \left[\rho_0^{(j)} v_0^{(j)}\frac{\partial U}{\partial y}\right]_1^2 = 0,$$

$$y = H^{(2)}: \quad U\frac{dH^{(2)}}{dx} = V, \quad \frac{\partial U}{\partial y} = 0. \qquad [5]$$

This approximation is similar to that used in the theory of a boundary layer.

To formulate the problem of a stationary flow, system [5] is completed by the initial conditions at $x = 0$

$$H^{(1)} = h_0, \quad H^{(2)} = 1, \quad U^{(j)} = U_0^{(j)}(y), \quad j = 1, 2. \qquad [6]$$

For numerical solutions [5] and [6], the collocation method is applied, see Shkadov (1973) and Epikhin *et al.* (1989a). The results of computations show that the velocity of the jet flow tends asymptotically to uniform distribution across jet sections with the growth of x independently of the initial velocity profile $U_0^{(j)}, j = 1, 2$.

As an example, let us consider a jet in which the first fluid is water and the second is benzene ($\rho_0 = 0.752$, $v_0 = 0.709$, $\sigma_0 = 1.5$) for the case Re = 100, We = 20. For the initial profile

$$U_0^{(j)} = 3\beta^{(j)} y^2 (0.5y^2 - 1) + \epsilon^{(j)}, \quad j = 1, 2,$$

$$\beta^{(2)} = \frac{\epsilon^{(2)} - 1}{1 - (1 - \rho_0 v_0) h_0^4 (h_0^2 - 1.5)}, \quad \beta^{(1)} = \rho_0 v_0 \beta^{(2)},$$

$$\epsilon^{(1)} = \epsilon^{(2)} + 3(1 - \rho_0 v_0) h_0^2 (0.5h_0^2 - 1)\beta^{(2)} \qquad [7]$$

at $\epsilon^{(2)} = 3$, $h_0 = 0.5$ two examples of stationary flows are depicted in figure 1 where definitions of mean axial velocities are used

$$U_m^{(1)} = \frac{2}{(H^{(1)})^2}\int_0^{H^{(1)}} yU^{(1)}\,dy, \quad U_m^{(2)} = \frac{2}{(H^{(2)})^2 - (H^{(1)})^2}\int_{H^{(1)}}^{H^{(2)}} yU^{(2)}\,dy.$$

For the case Fr = 1 in figure 2, velocity profiles at some jet sections are presented.

It should be noted that problem [5], [6] has solutions as a uniform flow, i.e. a flow with a constant velocity profile at a jet cross section, in the cases

(a) $Fr = \infty$,

(b) $Fr \neq \infty, \quad \rho_0 < 1, \sqrt{q^{(1)}} = \dfrac{\rho_0}{\sigma_0(1 - \rho_0)}$

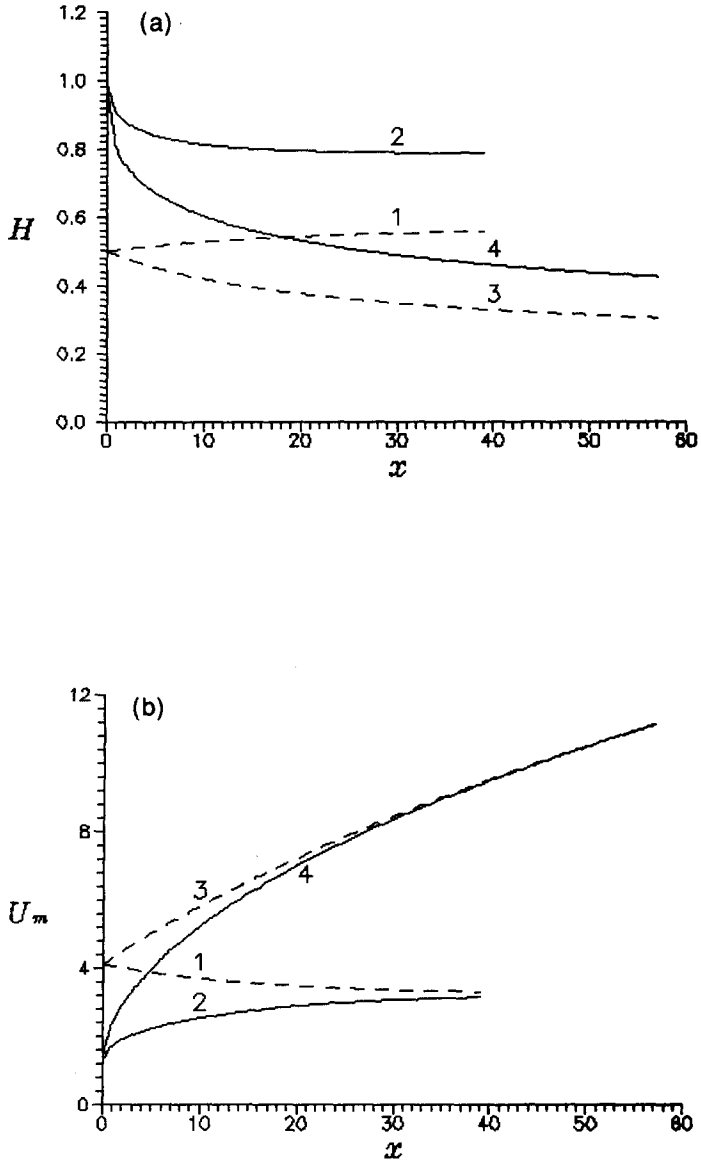

Figure 1. Stationary flows at Fr = ∞ (curves 1 and 2) and Fr = 1 (curves 3 and 4). Curves 1 and 3 correspond to $H^{(1)}$ or $U_m^{(1)}$, 2 and 4 to $H^{(2)}$ or $U_m^{(2)}$.

where

$$q^{(1)} = 2\int_0^{h_0} yU_0^{(1)}\,dy$$

is the rate of the first layer. This solution is represented as

$$H^{(1)} = H^{(2)}\sqrt{q^{(1)}}, \quad U = \frac{1}{(H^{(2)})^2}, \quad V = \frac{y}{(H^{(2)})^3}\frac{dH^{(2)}}{dx}$$

and the jet radius $H^{(2)}$ is defined by the equation

$$\frac{1}{2}\left(\frac{1}{(H^{(2)})^4} - 1\right) + \frac{\sigma_0}{\rho_0 \mathrm{We}}\left(\frac{1}{H^{(2)}} - 1\right) = \frac{x}{\mathrm{Fr}^2}.$$

This means that a uniform flow is possible at a gravityless case (a) or at a unique rate of inner layer (b). The impossibility of uniform flow in other cases is connected with the compounded act

of gravity and capillary forces. Gravity accelerates a flow along the x-direction which leads to $H^{(1)}$ and $H^{(2)}$ variation as follows from the kinematic conditions in [5]. The resulting curvatures of the interface and surface produce two different capillary forces $F^{(1)}$ and $F^{(1)}$. Case (b) corresponds to the equality of these forces.

In other cases, computation results show that the velocity profiles at the cross section approach uniform values in each layer as a result of viscous force effects at an initial region of x. As follows from velocity continuity at the interface, an area from close to it in which the velocity is varied. Across this vicinity one layer accelerates the other and vice versa. With an increase of the x-coordinate, mean velocities are approached in the layers. Thus at $x \to \infty$ a velocity profile approximates uniform flow.

4. THE STABILITY ANALYSIS

To investigate the stability of a stationary flow the assumption of its local plane-parallel feature is applied according to which the ratio of a typical scale along the x-coordinate for the perturbations to the corresponding scale of the main flow is assumed to be small, see Shkadov (1973). The assumption allows disregardance of the radial velocity and the variations of the main flow characteristics near some axial coordinate value x_*, where the growth of small perturbations is studied. For stability analysis the non-stationary solution is represented in the form

$$u(x, y, t) = U(x_*, y) + u_1(\xi, \eta, \tau), \quad v = v_1, \quad p = p_1,$$
$$h^{(1)}(x, t) = H_*[h_* + h_1^{(1)}(\xi, \tau)], \quad h^{(2)} = H_*(1 + h_1^{(2)}) \qquad [8]$$

where $H_* = H^{(2)}(x_*)$, $\xi = (x - x_*)/H_*$, $\eta = y/H_*$, $\tau = t/H_*$, $h_* = H^{(1)}(x_*)/H_*$.

After substitution of [8] into [1], linearizing the resulting equations with respect to the small perturbations and considering solutions of the form $f(\eta)\exp i\alpha(\xi - c\tau)$, we obtain in each of the layers

$$w_1' = \frac{w_4}{\eta}, \quad w_2' = -\alpha w_1 - \frac{w_2}{\eta},$$
$$w_3' = \rho_0^{(j)}\eta\alpha\left(U - c - \frac{i\alpha\nu_0^{(j)}}{\mathrm{Re}_*}\right)w_2 + \frac{w_3}{\eta} - \frac{i\alpha\rho_0^{(j)}\nu_0^{(j)}}{\mathrm{Re}_*}w_4,$$
$$w_4' = \alpha\eta\left[\alpha + \frac{i\mathrm{Re}_*}{\nu_0^{(j)}}(U - c)\right]w_1 + \frac{i\mathrm{Re}_*}{\nu_0^{(j)}}\left(\eta U' w_2 + \frac{\alpha}{\rho_0^{(j)}}w_3\right) \qquad [9]$$

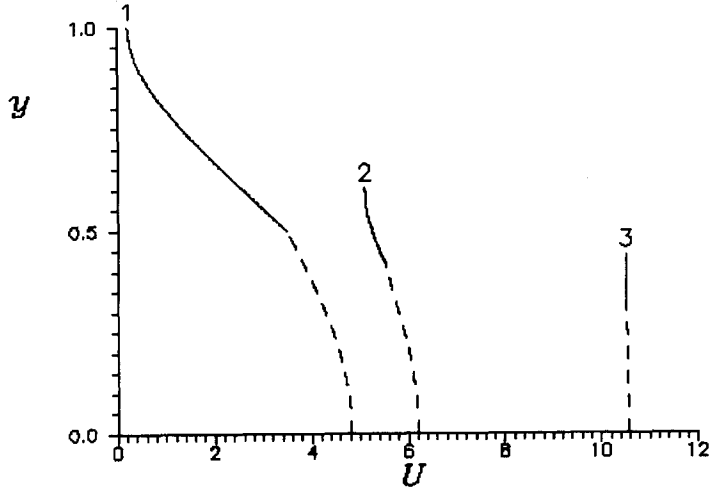

Figure 2. Velocity profiles at $x = 0$ (curve 1), 10 (curve 2) and 50 (curve 3). The dashed lines correspond to the first layer and the continuous lines to the second layer.

where $\mathrm{Re}_* = \mathrm{Re}\, H_*$ and functions $w_1(\eta), \ldots, w_4(\eta)$ are connected with amplitudes of variables by the relations $w_1 = u, w_2 = -iv, w_3 = \eta p, w_4 = \eta u'$. The prime in [9] and below symbolizes the differentiation with respect to the variable η.

The linearized boundary conditions at the interface are rewritten in the form

$$\eta = h_*: \quad \left[w_1 + \frac{U'}{\alpha(U-c)} w_2\right]_1^2 = 0, \quad [w_2]_1^2 = 0,$$

$$\left[2i\frac{\rho_0^{(j)} \nu_0^{(j)}}{\mathrm{Re}_*}\left(\alpha h_* w_1 + \left(1 + \frac{h_* U'}{U-c}\right) w^2\right) + w_3\right]_1^2 - \frac{1-(\alpha h_*)^2}{\sigma \mathrm{We}_* h_* (U-c)} w_2 = 0,$$

$$\left[\rho_0^{(j)} \nu_0^{(j)}\left(h_*\left(\frac{U''}{\alpha(U-c)} - \alpha\right) w_2 + w_4\right)\right]_1^2 = 0 \qquad [10]$$

where $\mathrm{We}_* = \mathrm{We}\, H_*$.

At the jet surface we obtain the relations

$$\eta = 1: \quad w_1 + \frac{1}{\alpha}\left\{1 - \frac{1}{\alpha(U-c)}\left[\frac{i\,\mathrm{Re}_* \sigma_0}{2\rho_0 \nu_0 \mathrm{We}_*}(1-\alpha^2) - \alpha U'\right]\right\} w_2 - \frac{i\,\mathrm{Re}_*}{2\alpha\rho_0\nu_0} w_3 = 0,$$

$$\left[\frac{U''}{\alpha(U-c)} - \alpha\right] w_2 + w_4 = 0. \qquad [11]$$

In the case of spatial periodic perturbations, [9] and the boundary conditions [10] and [11] form for bounded solutions the eigenvalue problem for c; the stability of the main flow is determined by the sign of c_i (here and henceforth the subscripts i and r mark the imaginary and real parts of the corresponding expression). In this problem the role of parameters is played by ρ_0, ν_0, σ_0, Re_*, We_*, h_*.

To solve the problem the numerical method is used according to which two linearly independent solutions are determined in the regions of both layers. For determination of these solutions near $\eta = 0$ they are represented in the form

$$w_{k(n)}^{(1)} = \sum_{m=0}^{\infty} w_{k(n)(m)}^{(1)} \eta^m, \quad k = 1, \ldots, 4, \quad n = 1, 2 \qquad [12]$$

see Lessen & Paillet (1974). After substitution of [12] into [9] one can define two independent solutions; the series [12] up to $O(\eta^2)$ are

$$\text{(a)} \quad w_{1(1)}^{(1)} = 1, \quad w_{2(1)}^{(1)} = -\frac{\alpha}{2}\eta, \quad w_{3(1)}^{(1)} = 0, \quad w_{4(1)}^{(1)} = 0,$$

$$\text{(b)} \quad w_{1(2)}^{(1)} = 1, \quad w_{2(2)}^{(1)} = 0, \quad w_{3(2)}^{(1)} = 0, \quad w_{4(2)}^{(1)} = 0, \qquad [13]$$

For $j = 1$, [9] with initial conditions [13] at some η close to zero are integrated up to $\eta = h_*$, the orthonormalization being performed at the interior points, see Godunov (1961). For $\eta = 1$ the following set of initial conditions satisfying [11] is used

$$\text{(a)} \quad w_{1(1)}^{(2)} = 0, \quad w_{2(1)}^{(2)} = 1,$$

$$w_{3(1)}^{(2)} = -\frac{2i\rho_0\nu_0}{\mathrm{Re}_*}\left\{1 - \frac{1}{U-c}\left[\frac{i\,\mathrm{Re}_* \sigma_0}{2\alpha\rho_0\nu_0 \mathrm{We}_*}(1-\alpha^2) - U'\right]\right\},$$

$$w_{4(1)}^{(2)} = \alpha - \frac{U''}{\alpha(U-c)},$$

$$\text{(b)} \quad w_{1(2)}^{(2)} = \frac{i\,\mathrm{Re}_*}{2\alpha\rho_0\nu_0}, \quad w_{2(2)}^{(2)} = 0, \quad w_{3(2)}^{(2)} = 1, \quad w_{4(2)}^{(2)} = 0. \qquad [14]$$

Equations [9] for $j = 2$ with initial conditions [14] are integrated up to $\eta = h_*$ also. The characteristic equation for the determination of eigenvalues is defined by [10] and has the form

$$\det \| L_{mn} \| = 0 \qquad [15]$$

where matrix elements are represented as

$$L_{1,n+2(j-1)} = (-1)^j\left[w^{(j)}_{1(n)} + \frac{U'}{\alpha(U-c)}w^{(j)}_{2(n)}\right],$$

$$L_{2,n+2(j-1)} = (-1)^j w^{(j)}_{2(n)},$$

$$L_{3,n+2(j-1)} = (-1)^j\left\{\frac{2i\rho_0^{(j)}\nu_0^{(j)}}{\mathrm{Re}_*}\left[\alpha h_* w^{(j)}_{1(n)} + \left(1 + \frac{h_* U'}{U-c}\right)w^{(j)}_{2(n)}\right] + w^{(j)}_{3(n)}\right\}$$
$$+ (j-2)\frac{1-(\alpha h_*)^2}{\alpha\,\mathrm{We}_* h_*(U-c)}w^{(j)}_{2(n)},$$

$$L_{4,n+2(j-1)} = (-1)^j\rho_0^{(j)}\nu_0^{(j)}\left[\frac{h_*}{\alpha}\left(\frac{U''}{U-c} - \alpha^2\right)w^{(j)}_{2(n)} + w^{(j)}_{4(n)}\right\}, \quad n, j = 1, 2. \qquad [16]$$

The values of the functions in [16] are calculated at $\eta = h_*$. The roots of [15] are defined by Newton's method.

5. DISCUSSION OF THE RESULTS

By varying the initial conditions in [6] it is possible to obtain different solutions of the problem of steady-state flow. The described numerical method of the stability analysis is suitable for computation of stability parameters, namely lengths, velocities and amplification factors of unstable waves, at any values x. It allows definition of the wave with a maximal growth rate at a fixed jet cross section and calculation of wave parameter variation along x. Because the stability problem is defined by six governing parameters: ρ_0, ν_0, σ_0, Re_*, We_* and h_*, the complete investigation in their space requires an unacceptable volume of computations. Below, the effects of the parameters are demonstrated by means of cases in which one of the governing parameters is varied while the others remain fixed. As the basis for investigation, the parameters of the water–benzene system are used. To carry out stability analysis, jet flows with certain given velocity profiles are considered.

For the case $U(\eta) = 1$ the stability of a compound jet has been studied in the papers mentioned in the Introduction. Two types of instability disturbances have been found. The first corresponds to the interface between the layers and the second relates to the jet surface. For inviscid fluids in the case of large We_*, the disturbances of the second type dominate, see Radev & Shkadov (1985), Kamenov & Radev (1987) etc. and this conclusion is confirmed for a viscous jet (Kamenov & Radev 1988). For example, in figure 3 results are depicted for two values of We_* at $\sigma_0 = \mathrm{We}_*/13.3$ which connect to variation $\sigma^{(1)}$ at $\sigma^{(2)} = \mathrm{const}$. (In the figure the dashed and continuous curves correspond

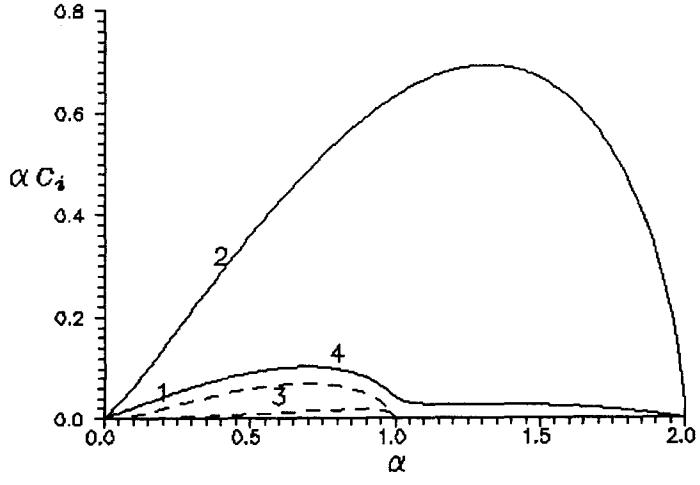

Figure 3. Amplification factors in the case $h_* = 0.5$, $\rho_0 = 0.752$, $\nu_0 = 0.709$, $\mathrm{Re}_* = 100$ and $U = 1$. Curves 1 and 2 correspond to $\mathrm{We}_* = 1.33$, curves 3 and 4 to $\mathrm{We}_* = 133$.

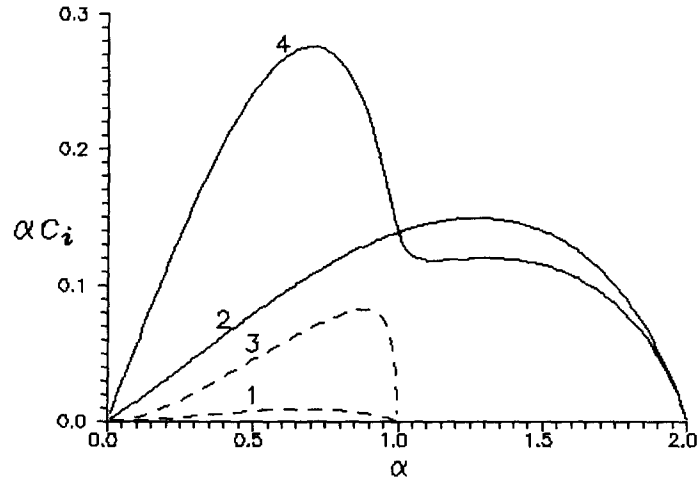

Figure 4. Amplification factors in the case $h_* = 0.5$, $\rho_0 = 0.752$, $\nu_0 = 0.709$, $\mathrm{Re}_* = 100$, $\mathrm{We}_* = 20$ and $U = 1$. Curves 1 and 2 correspond to $\sigma_0 = 0.1$, curves 3 and 4 to $\sigma_0 = 10$.

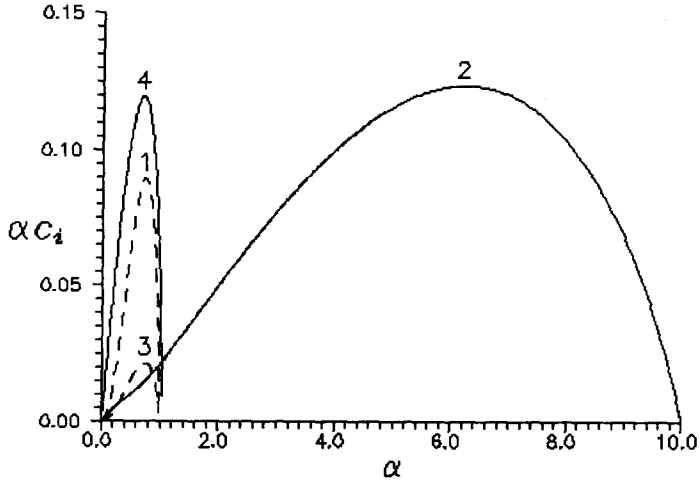

Figure 5. Amplification factors in the case $\rho_0 = 0.752$, $\nu_0 = 0.709$, $\sigma_0 = 1.5$, $\mathrm{Re}_* = 100$, $\mathrm{We}_* = 20$ and $U = 1$. Curves 1 and 2 correspond to $h_* = 0.1$, curves 3 and 4 to $h_* = 0.9$. The values of αc_i of curves 2 and 3 are multiplied by 0.1 and 10, respectively.

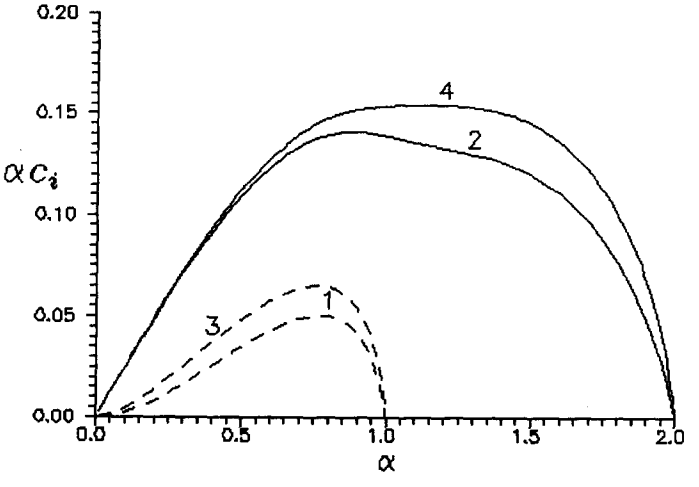

Figure 6. Amplification factors in the case $h_* = 0.5$, $\rho_0 = 0.752$, $\nu_0 = 0.709$, $\sigma_0 = 1.5$, $\mathrm{We}_* = 20$ and $U = 1$. Curves 1 and 2 correspond to $\mathrm{Re}_* = 100$, curves 3 and 4 to $\mathrm{Re}_* = 200$.

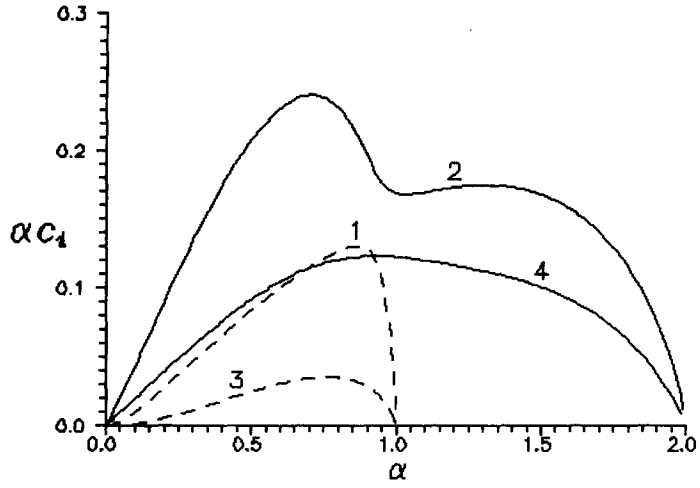

Figure 7. Amplification factors in the case $h_* = 0.5$, $v_0 = 0.709$, $\sigma_0 = 1.5$, $\mathrm{Re}_* = 100$ and $\mathrm{We}_* = 20$ and $U = 1$. Curves 1 and 2 correspond to $\rho = 0.1$, curves 3 and 4 to $\rho_0 = 1.4$.

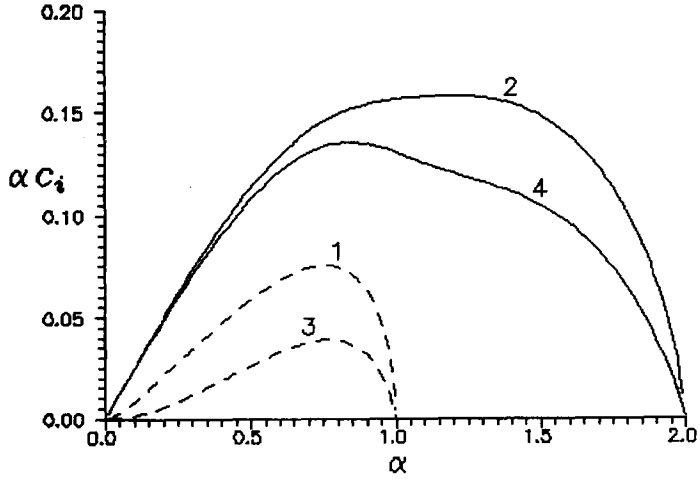

Figure 8. Amplification factors in the case $h_* = 0.5$, $\rho_0 = 0.752$, $\sigma_0 = 1.5$, $\mathrm{Re}_* = 100$, $\mathrm{We}_* = 20$ and $U = 1$. Curves 1 and 2 correspond to $v_0 = 0.1$, curves 3 and 4 to $v_0 = 1.4$.

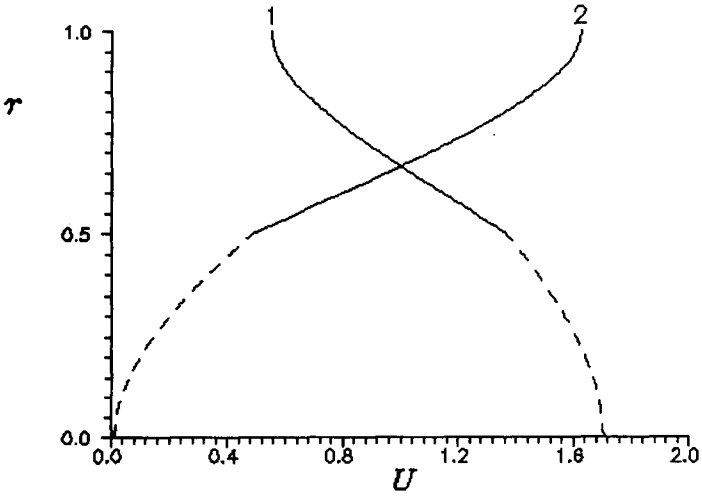

Figure 9. Velocity profiles U at $\epsilon^{(2)} = 2$ (curve 1) and $\epsilon^{(2)} = -0.4$ (curve 2) in the case $h_* = 0.5$, $\rho_0 = 0.752$, $v_0 = 0.709$.

to interface type disturbances and surface type disturbances, respectively.) Also note the predominance of the surface disturbances for finite values of We_*.

The examples of σ_0 variations which correspond to various $\sigma^{(2)}$ at $\sigma^{(1)} = \text{const.}$ are shown in figure 4. It can be seen that the maxima of the amplification factors for disturbances of both types are increasing with σ_0 growth and the surface perturbation are more dangerous.

The effect of the relative thickness factor is illustrated in figure 5. The essential predominance of the surface instability modes in the case of the thin first layer can be noted here. An increase of the amplification factor in accordance with Re_* variations for disturbances of both types is shown in figure 6. The decrease of the amplification factor with the increase of ρ_0 (or $\rho^{(2)}$) and ν_0 (or $\nu^{(2)}$) is shown in figures 7 and 8. One notes that the wave velocity $c_r = 1$ for disturbances of both types at $U = 1$. The aforementioned results on the instability of jet flows with constant velocity $U = 1$ are in accordance with the conclusions of Radev & Shkadov (1985), Kamenov & Radev (1988) and Radev & Tchavdarov (1988).

The examples of stability characteristics calculation for the non-uniform velocity profile U given by [7] at $\epsilon^{(2)} = 2$ and $h_0 = h_*$ (figure 9) are depicted below. Use of a main flow velocity in the form [7] is for two reasons. One is connected with the parabolic velocity profile of a jet at the output section of a nozzle, see Hertz & Hermanrud (1983). To satisfy the boundary conditions from [5] it is necessary to replace the parabolic profile in [7]. It may be noted that the stability analysis results based on [7] lose accuracy at $\alpha \to \infty$ because the local velocity distribution [7] is not the solution of [5] for all x. The other reason is that the velocity profile [7] allows consideration of the instability mechanism related with the discontinuity of a velocity gradient dU/dy at the interface between layers. This instability mechanism was studied in Hooper & Boyd (1983). The relative role of the instability mechanism connected with the discontinuity of the velocity gradient and with the capillary waves will be demonstrated below. A similar situation occurs in the case of a two-layer film flowing down an inclined plane. The wave formation at the interface of the films is connected with shear flow instability and with the capillary instability, as was shown in Sisoev & Shkadov (1992).

Let us repeat previous computations for a non-uniform velocity profile. The variation of We_* for $We_*/\sigma_0 = \text{const.}$ which corresponds to different values of $\sigma^{(1)}$ shows a non-essential effect on the growth rate of surface type waves (figure 10). A decrease of the interface tension $\sigma^{(1)}$, which corresopnds to the growth of We_*, leads to stabilization of the interface type waves which is usual for capillary instability. Unlike figure 3, the interface waves dominate for finite values of We_*.

Figure 11 demonstrate the effect of σ_0 which can be in interpreted as $\sigma^{(2)}$ variation at other fixed physical parameters. Unlike the case of figure 4, at small σ_0 the maximum growth rate of the interface waves is larger than the corresponding value of the surface waves. The surface type

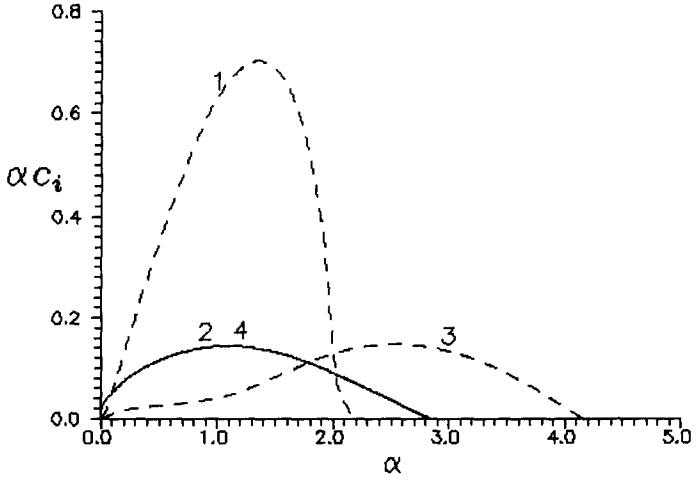

Figure 10. Amplification factors in the case $h_* = 0.5$, $\rho_0 = 0.752$, $\nu_0 = 0.709$, $Re_* = 100$, $\sigma_0 = We_*/13.3$ and velocity profile U at $\epsilon^{(2)} = 2$. Curves 1 and 2 correspond to $We_* = 1.33$, curves 3 and 4 to $We_* = 133$.

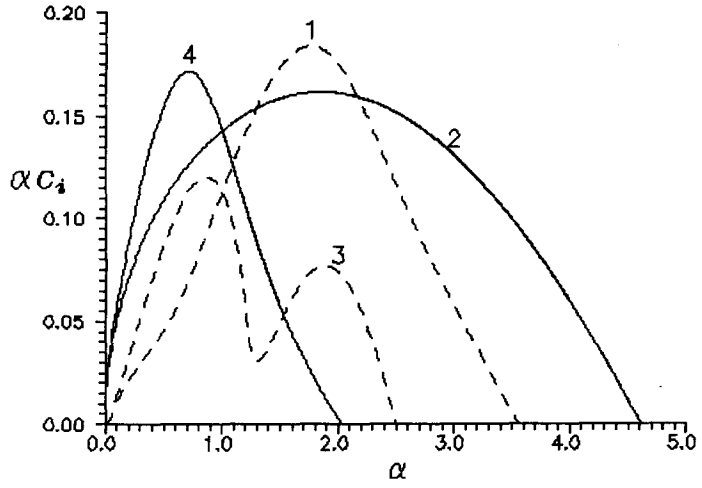

Figure 11. Amplification factors in the case $h_* = 0.5$, $\rho_0 = 0.752$, $\nu_0 = 0.709$, $\mathrm{Re}_* = 100$ and $\mathrm{We}_* = 20$ and velocity profile U at $\epsilon^{(2)} = 2$. Curves 1 and 2 correspond to $\sigma_0 = 0.1$, curves 3 and 4 to $\sigma_0 = 10$.

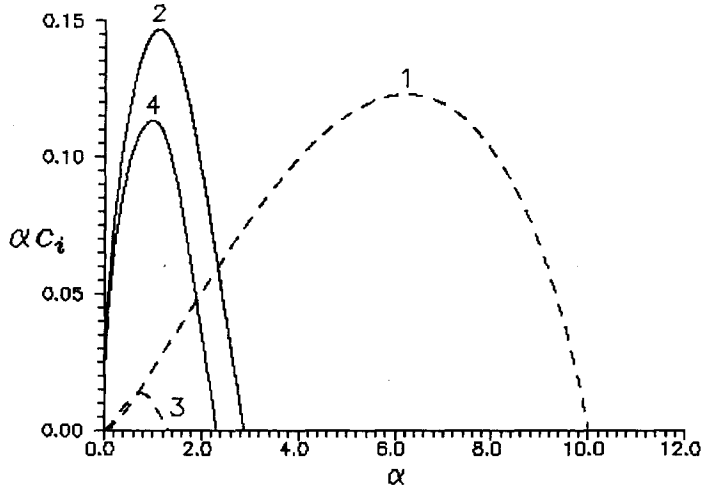

Figure 12. Amplification factors in the case $\rho_0 = 0.752$, $\nu_0 = 0.709$, $\sigma_0 = 1.5$, $\mathrm{Re}_* = 100$, $\mathrm{We}_* = 20$ and velocity profile U at $\epsilon^{(2)} = 2$. Curves 1 and 2 correspond to $h_* = 0.1$, curves 3 and 4 to $h_* = 0.9$. Values of αc_i of curve 1 are multiplied by 0.1.

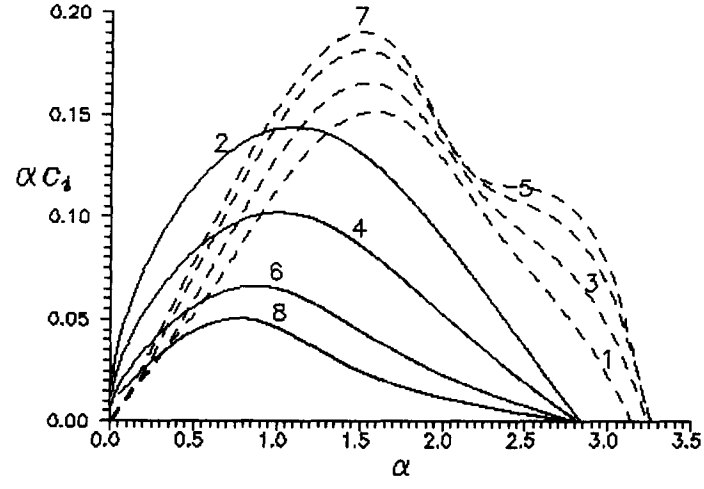

Figure 13. Amplification factors in the case $h_* = 0.5$, $\rho_0 = 0.752$, $\nu_0 = 0.709$, $\sigma_0 = 1.5$, $\mathrm{We}_* = 20$ and velocity profile U at $\epsilon^{(2)} = 2$. Curves 1 and 2 correspond to $\mathrm{Re}_* = 100$, curves 3 and 4 to $\mathrm{Re}_* = 200$, curves 5 and 6 $\mathrm{Re}_* = 500$, curves 7 and 8 to $\mathrm{Re}_* = 1000$.

perturbations become most dangerous as the value of σ_0 grows. In previous works of Kamenov & Radev (1987, 1988), Radev & Tchavdarov (1988) only the amplification factor curves with two local maxima for the surface type perturbations have been obtained.

Figure 12 presents the calculation results for two values of h_*. Unlike figure 5 in the case of the thin first layer, the interface waves predominate. As follows from figures 5 and 12 at $h_* = 0.1$, the velocity profile variation distinguishing these cases and corresponding with the small rate variation in layers, namely $q^{(1)} = 0.01$ and $q^{(1)} = 0.02$, respectively, leads to a drastic effect on the amplification factor curves. This can be treated as the shear flow instability effect.

The interface waves can also be more dangerous for different Re_* (figure 13). It can be noted that growth of the Re results in a stabilization effect on the surface type perturbations which differs from the case in figure 6.

The results of figure 14 confirm the effect of ρ_0 which are depicted in figure 7. Figure 14 demonstrates that the low-density jet cover perturbations of both types have comparable amplification factor maxima. Increase of the second layer density leads to the essential predominance of the surface type perturbation.

Unlike figure 8, in figure 15(a) predominance of the interface waves for $\nu_0 = 0.1$ is shown. It can be noted that increasing ν_0 leads to destabilization of the surface waves. Thus, increase of the external layer viscosity leads to predominance of surface type instability rather than interface instability. Wave velocities c_r are presented in figure 15(b). It can be noted that for waves of both types, the values of c_r are close to the main flow velocity at the interface or surface correspondingly and this is common for all calculations.

One notes that in previous examples connected with variations of $\rho_0 \nu_0$ and h_*, results are given for various jet flow. Figure 16 shows the results of stability analysis for two sections of the jet flow depicted in figure 1 at $\mathrm{Fr} = \infty$. At $x = 0$ the interface waves are more dangerous but at $x = 100$ the surface waves dominate. This result demonstrates the essential role of the initial region of a flow.

Let us consider the case of quicker cover in comparison with the inner layer. The results for the velocity profile [7] at $\epsilon^{(2)} = -0.4$ (figure 9) are similar to the case $\epsilon^{(2)} = 2$. For example, figures 17 and 18 show the effects of the interface tension and the surface tension.

The presented results show that conditions of the jet formation define the dominant type of disturbance. This has been confirmed in the experiments, see Hertz & Hermanrud (1983), where two regimes of jet disintegration at a low volume rate of a jet have been observed. One is similar to a single-layer jet and relates to surface collapse. In the second regime the inside liquid disintegrates into drops before the jet surface is destroyed. The latter may be connected with the predominance of interface type waves. In the experiments the role of tension has been

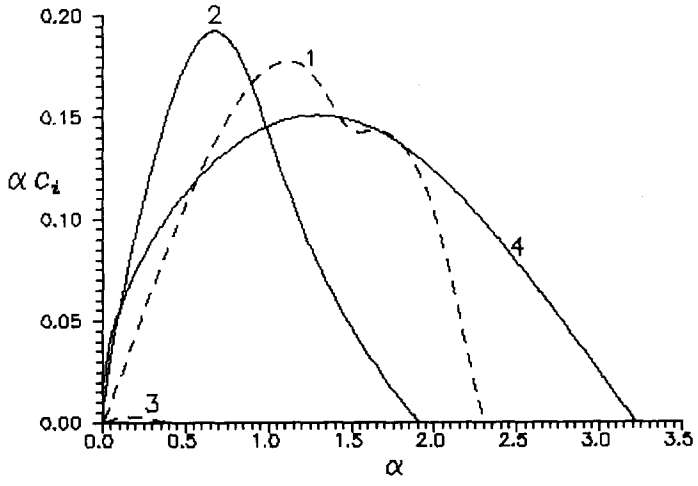

Figure 14. Amplification factors in the case $h_* = 0.5$, $\nu_0 = 0.709$, $\sigma_0 = 1.5$, $\mathrm{Re}_* = 100$, $\mathrm{We}_* = 20$ and velocity profile U at $\epsilon^{(2)} = 2$. Curves 1 and 2 correspond to $\rho_0 = 0.1$, curves 3 and 4 to $\rho_0 = 1.4$.

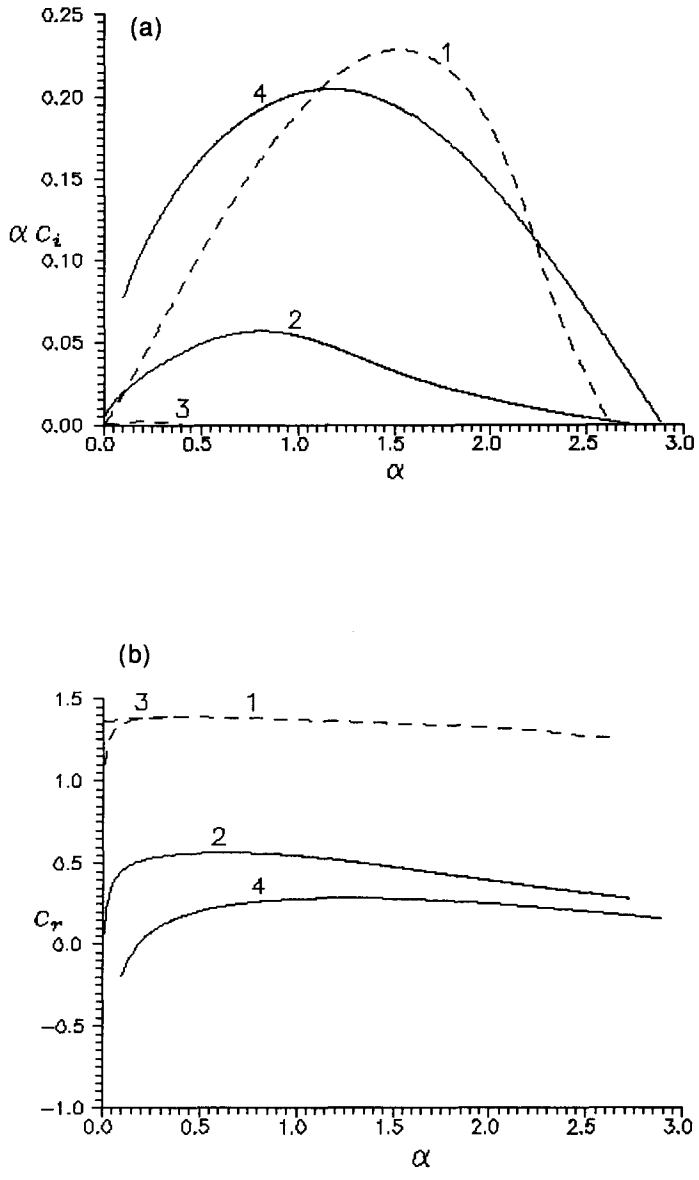

Figure 15. Amplification factors in the case $h_* = 0.5$, $\rho_0 = 0.752$, $\sigma_0 = 1.5$, $\mathrm{Re}_* = 100$, $\mathrm{We}_* = 20$ and velocity profile U at $\epsilon^{(2)} = 2$. Curves 1 and 2 correspond to $v_0 = 0.1$, curves 3 and 4 to $v_0 = 1.4$.

demonstrated, namely, at a large surface tension the jet breaks up by the first method, in accordance with the results in figure 11, and an increase of interface tension determines the disintegration of the inside layer much faster than the compound jet itself (figure 10).

For estimation of the jet disintegration regimes Radev & Shkadov (1985), Sanz & Meseguer (1985) and other investigators have used the results of linear instability analysis. They have considered the case of a uniform main jet flow with $U = 1$ and surface type perturbations only. The above-given results show that it is necessary to also consider interface type perturbations and to take into account the non-uniformity of the main flow. This implies that accurate calculations of the amplification factors for various positions along the jet with a fixed disturbance wave number are needed. Such calculations for a single-layer capillary jet interacting with surroundings were accomplished in Epikhin & Shkadov (1978). The above-outlined methods make it possible for stationary flow calculations and stability analysis of compound jets to be carried out.

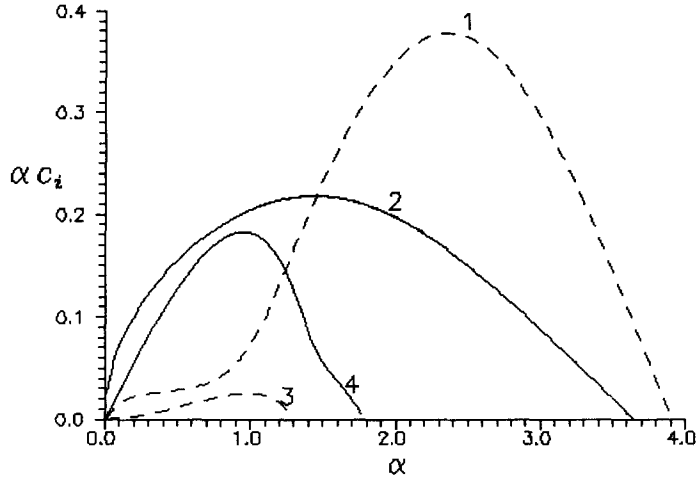

Figure 16. Amplification factors. Curves 1 and 2 correspond to $x = 0$, curves 3 and 4 to $x = 100$. The length scale of curves 3 and 4 is the same as at $x = 0$.

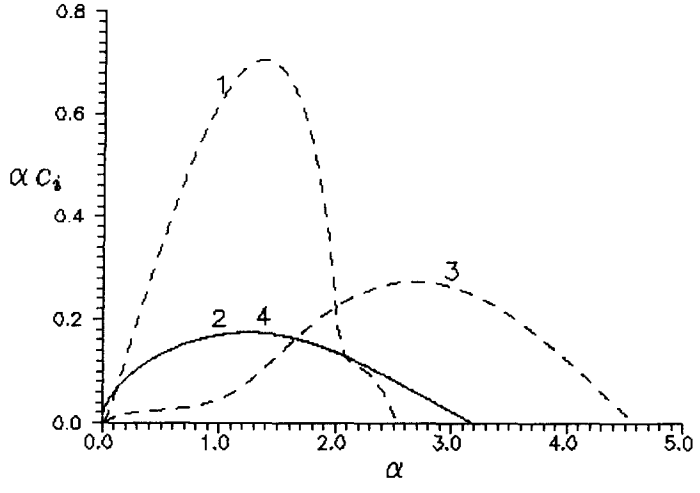

Figure 17. Amplification factors in the case $h_* = 0.5$, $\rho_0 = 0.752$, $\nu_0 = 0.709$, $\mathrm{Re}_* = 100$, $\sigma_0 = \mathrm{We}_*/13.3$ and velocity profile U at $\epsilon^{(2)} = -0.4$. Curves 1 and 2 correspond to $\mathrm{We}_* = 1.33$, curves 3 and 4 to $\mathrm{We}_* = 133$.

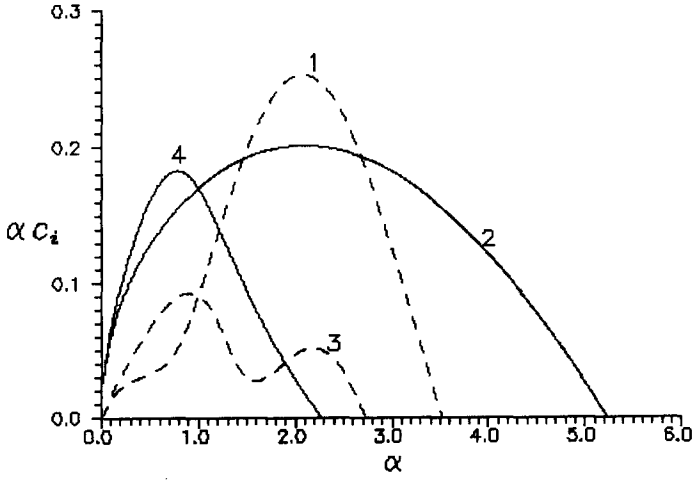

Figure 18. Amplification factors in the case $h_* = 0.5$, $\rho_0 = 0.752$, $\nu_0 = 0.709$, $\mathrm{Re}_* = 100$, $\mathrm{We}_* = 20$ and velocity profile U at $\epsilon^{(2)} = -0.4$ Curves 1 and 2 correspond to $\sigma_0 = 0.1$, curves 3 and 4 to $\sigma_0 = 10$.

6. CONCLUSIONS

The stability of a stationary axisymmetric flow of a two-layer capillary jet has been considered as the most common formulation. Two types of unstable axisymmetric disturbances, which relate to the interface between the layers and the jet surface, have been investigated. The dominant type of waves is defined by six governing parameters. The surface type perturbations dominate in the case of a uniform main flow velocity profile. Any other perturbation would be most dangerous if the velocity profile varies at the jet cross section. Numerous examples of the stability problem solution demonstrating the effects of the governing parameters and the main flow feature variations are presented.

Acknowledgement—This work was supported by the Russian Foundation of Fundamental Investigations, project number 94-01-01637.

REFERENCES

Duda, J. L. & Vrentas, J. S. 1967 Fluid mechanics of laminar liquid jets. *Chem. Engng Sci.* **22,** 855–869.

Epikhin, V. E. & Shkadov, V. Ya. 1978 Flow and instability of capilary jets interacting with surroundings. *Fluid Dynam.* **13,** 50–59.

Epikhin, V. E., Sisoev, G. M. & Shkadov, V. Ya. 1989a Stationary flow of compound capillary jets. *J. Appl. Mech. Tech. Phys.* **1,** 134–138.

Epikhin, V. E., Sisoev, G. M. & Shkadov, V. Ya. 1989b Flow of two-layer axysmmetric jets with initial twisting. *Moscow Univ. Mech. Bull.* **44,** 67–71.

Godunov, S. K. 1961 Numerical solution of boundary-value problems for systems of linear ordinary differential equations. *Uspek. Matemat. nauk* **16,** 171–174 (in Russian).

Hertz, C. H. & Hermanrud, B. 1983 A liquid compound jet. *J. Fluid Mech.* **131,** 271–287.

Hooper, A. P. & Boyd, W. G. C. 1983 Shear-flow instability at the interface between two viscous fluids. *J. Fluid Mech.* **128,** 507–528.

Kamenov, O. & Radev, S. 1987 Linear instability of two-layer inviscid capillary jet. *Theor. Appl. Mech.* **18,** 44–53 (in Bulgarian).

Kamenov, O. & Radev, S. 1988 Linear instability of viscous two-layer jet. *Theor. Appl. Mech.* **19,** 50–59 (in Bulgarian).

Lessen, M. & Paillet, F. 1974 The stability of trailing line vortex. Part 2. Viscous theory. *J. Fluid Mech.* **65,** 769–779.

Markova, M. P. & Shkadov, V. Ya. 1972 Nonlinear development of capillary waves in a liquid jet. *Fluid Dynam.* **7,** 30–37.

Petryanov-Sokolov, I. V. & Shutov, A. A. 1984 Capillary instability of a liquid jet with thin cover. *Sov. Phys. Dokl.* **276**(3), 576–578.

Radev, S. & Gospodinov, P. 1986 Numerical treatment of the steady flow of a liquid compound jet. *Int. J. Multiphase Flow* **12,** 997–1007.

Radev, S. & Shkadov, V. 1985 On a stability of two-layer capillary jet. *Theor. Appl. Mech.* **16,** 68–75.

Radev, S. & Tchavdarov, B. 1988 Linear capillary instability of compound jets. *Int. J. Multiphase Flow* **14,** 67–79.

Sanz, A. & Meseguer, J. 1985 One-dimensional linear anlaysis of the compound jet. *J. Fluid Mech.* **159,** 55–68.

Shkadov, V. Ya. 1973 *Some Methods and Problems of the Theory of Hydrodynamic Stability.* Moscow University, Moscow (in Russian).

Shkadov, V. Ya., Radev, S. P. Penchev, I. P. & Gospodinov, P. N. 1982 Flow and instability of liquid capillary jets. *Adv. Mech.* **5**(3/4), 105–146 (in Russian).

Shutov, A. A. 1985 Instability of a liquid compound jet. *Fluid Dynam.* **20,** 3–8.

Sisoev, G. M. & Shkadov, V. Ya. 1992 Instability of two-layer film flow along an inclined plane. *Fluid Dynam.* **27,** 160–165.